SULFUR SPECIATION IN MURCHISON USING μ-XRF and μ-XANES. M. Bose[1] and R. Root[2], [1]Department of Chemistry and Biochemistry, Arizona State University, Tempe, AZ 85283-1604. [2]Department of Soil, Water & Environmental Science, University of Arizona. Tucson, AZ 85721-0038. E-mail: Mairayee.Bose@asu.edu.

Introduction: The insoluble organic matter (IOM) in Murchison is often described simplistically by the elemental formula $C_{100}H_{70}O_{22}N_3S_7$. Sulfur, which is an important addition to the C, H, N and O-containing components of the IOM is characteristically heterovalent, exhibiting a large range in oxidation state (-2 to +6) of the geochemically abundant elements, and readily forms chemical bonds with both electropositive and electronegative elements. The speciation of sulfur and relative contents of the sulfur-bearing phases in carbonaceous chondrites is critical to understand the nature and extent of post-accretion processes that affected the matrices of these chondrites in the early solar system. Both the reduced and oxidized forms of sulfur have been identified in carbonaceous chondrites [1, 2]. Sulfide minerals are ubiquitous in chondrites, while the occurrence of sulfate minerals typically indicates aqueous alteration in the asteroid parent bodies [3]. The IOM, primarily in the matrix of the meteorites is more susceptible to aqueous alteration, and can be a more sensitive indicator of this alteration process than the minerals themselves. In addition, S-bearing organic compounds may have been produced on mineral grains in the nebular phase so this study attempts to distinguish these species.

The chemical nature of the sulfur-bearing species in IOM ascertained from two carbonaceous chondrites, Murchison and Allende were reported in [4]. With an informed view of the sulfur compunds present in Murchison, a thin section of Murchison was mapped for S compounds by μ–XRF and point spectra on the same field of view was acquired to corroborate the mapped data.

Methods:

IOM Extraction and hydrothermal treatment: The IOM was extracted from two carbonaceous chondrites Murchison and Allende. Hydrothermal treatment was done at 300°C and 100MPa pressure for 6 days [5].

XANES: Bulk speciation from extracted IOM was interrogated with XANES at beam line 4-3, at the Stanford Synchrotron Radiation Lightsource (SSRL), a National Laboratory user facility operated by the DOE. The x-ray beam was operated at 3 GeV and 500 mA with a double-crystal monochromator (Si [220] crystal, ϕ= 90) used to tune the incident energy on the sample. The full beam was slit down to 2 (vertical) x 10 (horizontal) mm with the sample at a 45 degree angle to the beam. To minimize the effect of self-absorption powdered samples were deposited as a monolayer of fine particles (<20 μm) on S-free polyimide tape (Kapton) and analyzed under a He atmosphere using a passivated implanted planar silicon (PIPS) fluorescence detector. Energy was calibrated between each set of sample scans using the centroid of the first peak of sodium thiosulfate, assigned to 2472.02 eV.

The average of 6 scans was normalized using the software package ATHENA (Ravel), i.e. the pre edge and post edge regions were flattened with a linear function, the pre-edge region was re-assigned to 0 and the post edge reassigned to 1. The speciation of S was determined with LCF by fitting the normalized 1s XANES from 2460 eV to 2510 eV using linear least-squares combinations of reference compound spectra with the computer package ATHENA (Ravel). XANES spectra were fit using 1. pyrite as the reduced sulfide model, 2. elemental sulfur, 3. cysteine, 4. dibenzothiophene, 5. methionine sulfone, 6. anthraquinone sulfonic acid, and 7. melaterite, selected from a suite of over fifty organic and inorganic sulfur reference spectra. The final seven model spectra were selected based on goodness of fit to the sample spectra and corroborating chemical information for the samples. Least squares LCF of sample spectra was fit by multiple iterations of reference components, generally >100 combinations. Components fit with an abundance fraction less than 1% were removed and the spectra were refit to determine if the addition of the low concentration phase significantly improved fit statistics.

Imaging with microXRF: Several multiple energy "maps" across the S absorption edge at 2471.1 eV, 2472.6 eV, 2473.5 eV, 2476.3 eV, 2481.3 eV, 2482.5 eV, 2482.7 eV, 2499.0 eV were collected for 6 areas on a thin section of a Murchison carbonaceous chondrite. Each energy was chosen to exploit a specific S oxidation state or species. Each S species will have a specific response at each energy mapped, which can be traced back to the S XANES. Putting the normalized fluorescence response into a matrix of energy v species gives a (nearly) pixel by pixel XANES (at the energies mapped, albeit with a lot of space between points). This has been sufficient for distinction of S species. To validate the maps, 10−16 μ-XANES spectra collected on specific points (~3 μm^2) of interest in each map that are used to collaborate the mapped species.

Results and Discussion: There are 5 primary groups in Murchison and Allende samples: sulfides, aliphatic S, heterocyclic S, oxidized S and sulfates. Murchison exhibits a very diverse suite of S compou

nds in this meteorite. As reported in [4], Murchison has both oxidized and reduced forms of S, while Allende's inventory is predominantly in the -1 to 0 oxidation states. The Murchison IOM samples (*Figure 1*) show peaks of exocyclic compounds such as alkyl and aryl disulfides and elemental S, heterocyclic compounds, aromatic rings of dibenzothiophene, and very prominent sulfate peak possibly sodium sulfate or magnesium sulfate. The presence of the small dimethyl sulfoxide peak is intrinsic to the sample because these samples were stored carefully in sealed containers. The hydrothermally altered IOM sample shows a peak for heterocycles while the IOM does not, and this most likely reflects the heterogeneity in the sample. Loss of disulfide, i.e. pyrite, and elemental S from the first peak and the appearance of the thiophene and sulfonyl features in the second peak in the IOM vs HT-IOM. Murchison also shows a small sulfite peak.

The Allende IOM on the other hand, shows peaks of elemental sulfur and alkyl sulfides. Thiophenes, sulphones and sulphonic acids are absent in Allende. This broad peak is not due to sulfones or sulfonyl reduced sulfur species) but is a post edge feature from constructive interference from multiple scattering events from S and near neighbor atoms (here likely another S), analogous to the broad feature at about 2495−2500 in the oxidized samples.

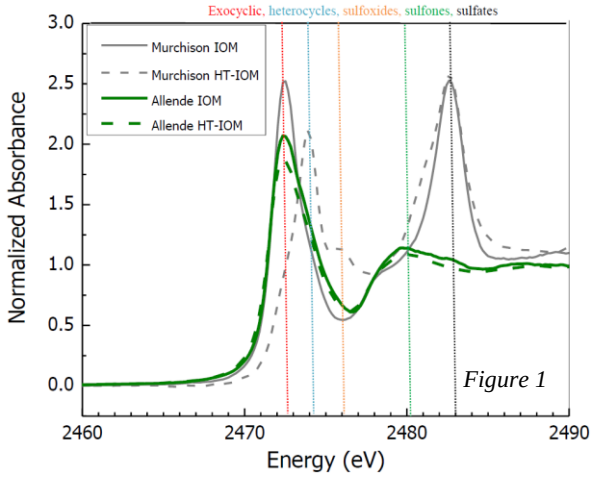

Figure 1: *Sulfur XANES spectra for Murchison (grey) and Allende samples (green) IOM and hydrothermally treated IOM samples. Vertical lines are the S peaks at specific K-edge binding energies.*

Knowing the suite of diverse S-bearing compounds in Murchison IOM, a thin section of Murchison (*Figure 2*) was probed to locate areas with different oxidation states. *Figure 3* illustrates the S heat map (abundance) and oxidation states for a rim around a calcium aluminum inclusion (CAI).

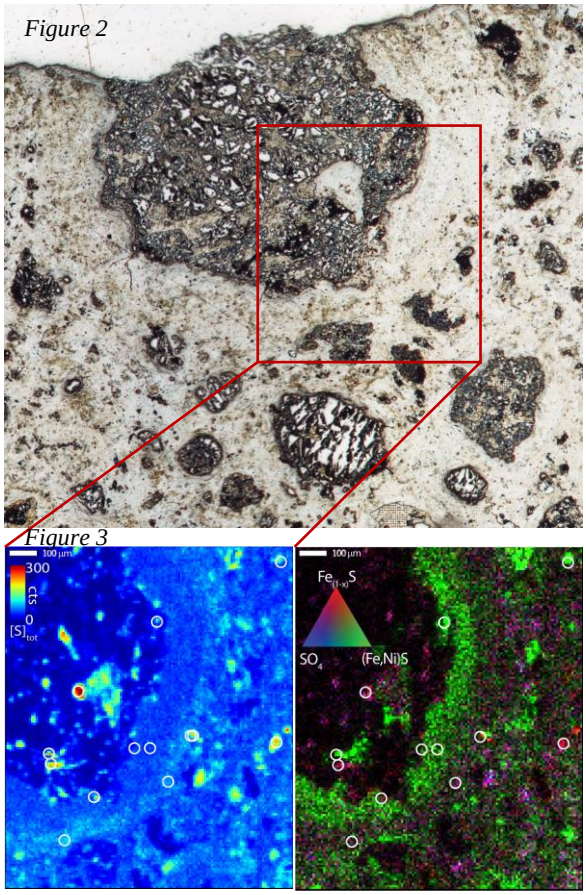

Figure 2 (top): *Light-microscope reflected image of an area around a CAI in Murchison. The area within the red box was further analyzed using µ-XRF and µ-XANES.* ***Figure 3 (left):*** *µ–XRF images of Murchison for total S.* ***Figure 3 (right):*** *Multiple energy stacked maps of S species showing FeS (red), (Fe,Ni)S (green), and SO_4 (blue). Circles indicate locations of µ-XANES used to confirm speciation determined with multiple energy maps; scale bar is 100 µm for both images.*

The Fe,Ni sulfides form a boundary layers around the CAI with smaller domains of pure FeS present. The purple, yellow, and teal colors are mixtures of the primary species, and show co-localization of multiple phases. Results from mapped regions around chondrules and the fine-grained matrix and implications from the data will be discussed at the meeting.

References: [1] Orthous-Daunay F. –R. et al. (2010) *Earth Planet. Sci. lett., 300*, 321−328. [2] Cooper G. W. et al. (1997) *Science, 277*, 1072−1074. [3] Burgess R. et al. (1991) *Meteoritics, 26*, 55−64. [4] Bose M. et al. (2015) 78th Meteoritics & Planetary Science, Abstract #5260. [5] Pizzarello S. and Williams L. (2012) *Astrophys. J., 749*, 161−167.

Acknowledgements: M. Bose would like to thank the NSF grant (PI R. Hervig; NSF EAR-1352996) for supporting her independent research and NASA grant (EOS NExSS; NNX15AD94G) for travel funds.